

# Interaction of supernova ejecta with circumstellar matter and X-ray emission: SN 1987A & SN 1993J

By T. SUZUKI, K. NOMOTO,  
T. SHIGEYAMA, AND S. KUMAGAI

University of Tokyo, Bunkyo-ku, Tokyo 113, Japan

We perform hydrodynamical calculations of the collision between the supernova ejecta and circumstellar matter for SN 1987A and SN 1993J. For SN 1987A we predict light curves of X-ray emissions from the shocked ring. For SN 1993J, thermal X-rays from the shocked circumstellar matter can consistently account for the observations with ROSAT, ASCA, and OSSE.

## 1. Introduction

The supernova ejecta collides with the circumstellar matter (CSM) if its progenitor was undergoing significant mass loss. Shock waves arising from this collision compress and heat the ejecta and the CSM. The emission from the shocked material strongly depends on the density distributions of the ejecta and the CSM, thereby providing important information about the nature of the CSM.

## 2. SN 1987A

The images from the European Southern Observatory (ESO) (Wampler *et al.* 1990) and the Hubble Space Telescope (HST) (Jakobsen *et al.* 1991) revealed the presence of a ring-like structure at  $\sim 6 \times 10^{17}$  cm from SN 1987A. The outermost part of the supernova ejecta is expanding at  $\sim 10^4$  km s $^{-1}$  (Shigeyama & Nomoto 1990), thus being expected to collide with the ring at  $\sim 10$  years after the explosion.

### 2.1. Hydrodynamical model

The progenitor of SN 1987A had once become a red supergiant (RSG) and then contracted to a blue supergiant (BSG) before the explosion (for reviews, see Arnett *et al.* 1989, Hillebrandt & Höflich 1989, Podsiadlowski 1992, and Nomoto *et al.* 1993a). This evolutionary scenario predicts that SN 1987A environment has been formed as follows: The progenitor blew a stellar wind with the velocity  $\sim 10$  km s $^{-1}$  and the mass loss rate  $\sim 10^{-5} M_{\odot}$  yr $^{-1}$  during the RSG stage, and with  $\sim 550$  km s $^{-1}$  and  $\sim 10^{-6} M_{\odot}$  yr $^{-1}$  during the BSG stage (Lundqvist & Fransson 1991). Consequently, the fast BSG wind struck the slow RSG wind, and a shock wave arising from this collision propagates outward through the RSG wind. The dense regions formed behind the shock wave by radiative cooling, which resulted in the high-density nebula. Formation of a ring as observed is due to, for example, the rotation of the progenitor or the magnetic field (Chevalier & Luo 1994; Washimi *et al.* 1994).

Our model consists of four components: the ejecta, the BSG wind, the RSG wind, and the ring (see Suzuki *et al.* 1993a for details). We adopt the model 14E1 by Shigeyama & Nomoto (1990) for the supernova ejecta, in which the density distribution in the outer envelope is power law as  $\rho \propto r^{-8.6}$ . We assume the density distributions of the BSG and RSG wind as  $\rho_{\text{BSG}}(r) = 9 \text{ amu cm}^{-3}$  at  $3 \times 10^{16} \text{ cm} < r < 5.7 \times 10^{17} \text{ cm}$  and

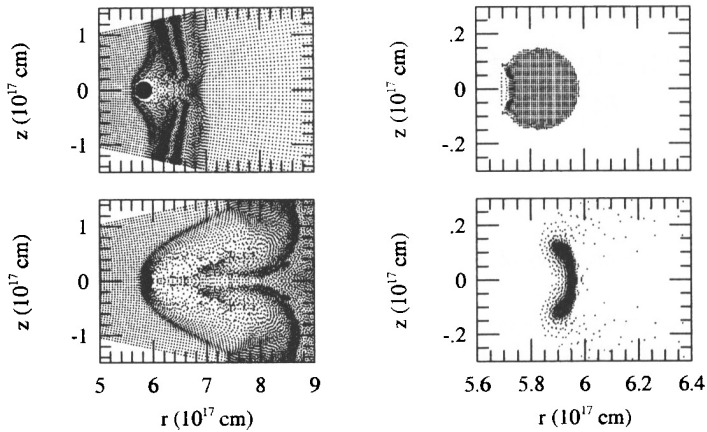


FIGURE 1. [left] Hydrodynamical evolution after the second collision. Shown are the configurations of particles at:  $t = 16$  yr (upper) and  $t = 36$  yr (lower). [right] Same as the left figures but the particles constituting the ring are plotted and the scale is magnified.

$\rho_{\text{RSG}}(r) = 3 \times 10^3 (r/10^{17} \text{ cm})^{-2} \text{ amu cm}^{-3}$  at  $r > 5.7 \times 10^{17} \text{ cm}$ , respectively. The ring is sunk in the RSG wind and touched to the contact surface between the spherical RSG and BSG winds. Here we adopt  $5.7 \times 10^{17} \text{ cm}$  for the distance from the supernova to the ring (Jakobsen *et al.* 1991; Panagia *et al.* 1991). We choose  $0.05 M_{\odot}$  and  $2.4 \times 10^4 \text{ amu cm}^{-3}$  respectively for the total mass and density of the ring (Lundqvist & Fransson 1991).

The expanding ejecta collides first with the BSG wind (*the first collision*). A shock wave generated by this collision propagates outward through the BSG wind and collides with the ring and the RSG wind (*the second collision*). We thus calculate the shock propagation from the first collision to the second collision with one-dimensional spherical Lagrangian Piecewise Parabolic Method (PPM) (Colella & Woodward 1984), and from the second collision with a two-dimensional cylindrical Smoothed Particle Hydrodynamics (SPH) (e.g., Benz 1990).

After the second collision three shock waves compress the ejecta, the RSG wind, and the ring, respectively (Fig. 1). When the shock wave reaches the edge of the ring at  $t \sim 36$  yr, the ring material is most strongly compressed and the X-ray emission reaches the maximum as will be described below.

## 2.2. X-ray emission

We calculate the X-ray emission due to thermal bremsstrahlung from the shocked material with assumption that the shocked material is completely ionized. Figure 2 shows the X-ray light curve. X-rays from the ring are dominant because of its high density. The luminosity increases monotonically as the mass of the shocked region increases. At  $t \sim 36$  yr when the shock wave reaches the edge of the ring, the ring is compressed most strongly, so that the luminosity attains its maximum of  $\sim 10^{37} \text{ erg s}^{-1}$ . Afterwards the luminosity decreases because the ring expands adiabatically to cool. The luminosity from the ejecta and the BSG wind also increases monotonically since the second collision. The luminosity from the RSG wind increases for several years, and levels because the shock wave propagates into lower density layers.

Our calculations have shown that the collision between the ejecta and the ring will start at  $\sim 12$ – $15$  years after the supernova explosion (see also Luo *et al.* 1994). The X-ray flux is predicted to reach the observable level with planned X-ray astronomical satellites. Detailed X-ray spectral predictions were made by Masai & Nomoto (1994).

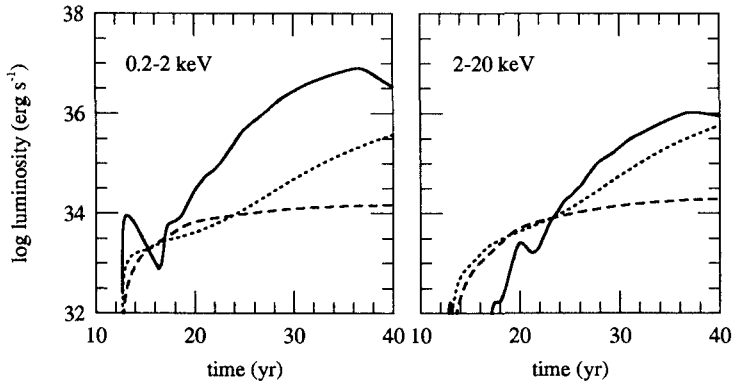


FIGURE 2. Calculated X-ray light curves of 0.2–2 keV (*left*) and 2–20 keV (*right*). Three lines indicate the components from the ring (*solid lines*), from the BSG wind and the ejecta (*dotted*), and from the RSG wind (*dashed*), respectively.

Then the future X-ray observations would provide critical information to diagnose the ring formation models (see Luo & McCray 1991, Wang & Mazzali 1992, and Lundqvist 1992).

### 2.3. X-rays observed with ROSAT

Recently, the positive detection of soft X-rays from SN 1987A with ROSAT has been reported (Gorenstein *et al.* 1994; Beuermann *et al.* 1994). The luminosity was  $\sim 10^{34}$  erg during 1991–1992. Compared with predictions by our hydrodynamical calculations and others (e.g., Itoh *et al.* 1992; Suzuki *et al.* 1993a; Luo *et al.* 1994; Masai & Nomoto 1994), the observed X-rays must originate from interactions of SN 1987A with the BSG wind matter and the inferred CSM density is  $20\text{--}30 \text{ amu cm}^{-3}$ . This density is higher than that used in our calculations, which implies slightly larger deceleration of the shock wave propagation and thus a slight delay of the onset of the collision with the ring.

Currently only the upper limit has been set by the ASCA observations (M. Itoh, private communication). Since our calculations predict the increase in the X-ray luminosity as the shock wave sweeps more CSM, it is likely that ASCA will observe X-rays from SN 1987A within its lifetime.

## 3. SN 1993J

X-ray emissions from SN 1993J have been observed from its early stages with ROSAT at 0.1–2.4 keV (Zimmermann *et al.* 1993) and ASCA at 1–10 keV (Tanaka *et al.* 1993). Suzuki *et al.* (1993b) have modeled the X-ray emissions by carrying out hydrodynamical calculations of the collision between the supernova ejecta and the CSM. Suzuki *et al.* (1993b) have found that the observed features of X-rays can be accounted for with thermal bremsstrahlung emission from the reverse-shocked ejecta, if the expansion velocity at the outer edge of the ejecta before the collision is as high as  $v_{\text{edge}} \sim 5 \times 10^4 \text{ km s}^{-1}$  and if the density gradient of the ejecta is relatively shallow ( $\rho \propto r^{-n}$  with  $n \sim 8$ ).

Recently Leising *et al.* (1994) have claimed that the OSSE on board Compton Observatory has detected hard X-rays from SN 1993J around day 10 and 35 after the explosion. The observed luminosity at 50–200 keV is  $\sim 5 \times 10^{40} \text{ erg s}^{-1}$  and the spectrum is approximately fitted to 90 keV thermal bremsstrahlung emission. The Comptonized hard X-rays due to the  $^{56}\text{Co}$  decays have been predicted to reach maximum around day 50 but the flux around day 10 is well below the detection limit for the  $0.07 M_{\odot} \text{ } ^{56}\text{Co}$  (Shigeyama

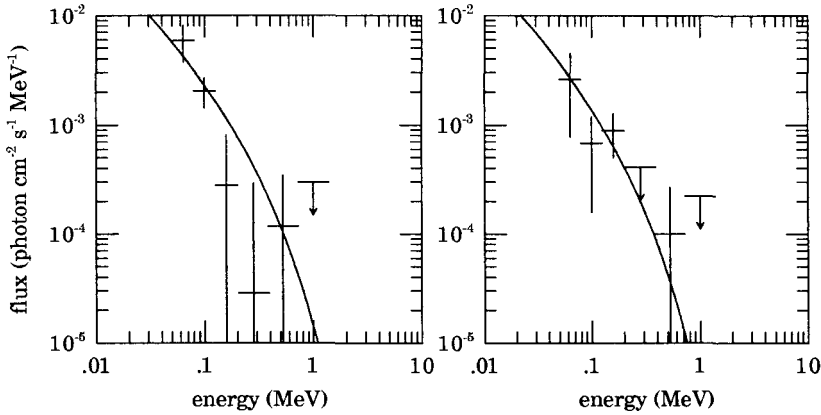


FIGURE 3. Calculated X-ray spectra at 10 (left) and 30 (right) days after the collision. Observations by OSSE during 9.9–15.4 (left) and 23.7–36.9 (right) days are plotted.

*et al.* 1994; Woosley *et al.* 1994). Compared with the calculated thermal emissions from the shocked ejecta (Suzuki *et al.* 1993b), the observed luminosity is much higher and the spectrum is much harder. These comparisons suggest that the observed hard X-rays are emitted from the shocked CSM rather than the ejecta (Leising *et al.* 1994).

### 3.1. Hydrodynamical model

Here we calculate the collision between the ejecta and the CSM for higher CSM densities than in Suzuki *et al.* (1993b). We also assume that the density distribution of the CSM is  $\rho = \rho_0(r/2 \times 10^{14} \text{ cm})^{-1.8}$  at  $r \geq 2 \times 10^{14} \text{ cm}$  rather than  $\propto r^{-2}$ , because the slow declines of the X-ray light curves observed with ROSAT (Zimmermann *et al.* 1994) and ASCA (Kohmura 1994) are better reproduced (see below). The outermost layer of ejecta is expanding homologously, so that its velocity distribution is  $v = v_{\text{edge}}(r/2 \times 10^{14} \text{ cm})$  and its density distribution is  $\rho = \rho_{\text{edge}}(r/2 \times 10^{14} \text{ cm})^{-n}$ . In this study  $\rho_{\text{edge}} = 3\rho_0$  is assumed (see Suzuki *et al.* 1993b).

The collision forms two shock waves: a forward shock propagating into the CSM and a reverse shock back into the ejecta. If the density gradient of the ejecta is as low as  $n \sim 8$ , the X-ray luminosity is dominated by the shocked ejecta because of higher densities in the ejecta than in the CSM. On the contrary, if the density gradient is as steep as  $n > 12$ , the shocked outer ejecta form a dense shell due to cooling which absorbs X-rays from the reverse-shocked ejecta. Here we assume  $n = 20$  as found in the hydrodynamical models for SN 1993J (Shigeyama *et al.* 1994), so that X-rays from the ejecta are absorbed by the dense shell. We also adopt  $v_{\text{edge}} = 5 \times 10^4 \text{ km s}^{-1}$  and  $\rho_0 = 1 \times 10^{-14} \text{ g cm}^{-3}$  which corresponds to  $\dot{M} = 8 \times 10^{-5} M_{\odot} \text{ yr}^{-1}$  for the wind velocity of  $10 \text{ km s}^{-1}$ . Since Coulomb collisions in the CSM are too slow to establish energy equipartition between electrons and ions, electron temperatures are significantly lower than ion temperatures. Yet, the electron temperatures in the CSM are still as high as  $\sim 3 - 6 \times 10^9 \text{ K}$  because of high shock speed.

### 3.2. X-ray emission

Figure 3 shows the calculated X-rays spectra of thermal bremsstrahlung emission from the shocked CSM at day 10 and 30, which are compared with the OSSE observations (Leising *et al.* 1994). Figure 4 shows the light curves of X-rays from the CSM compared with the ROSAT ( $L_{0.1-2.4}$ ) and ASCA ( $L_{1-10}$ ) observations and their ratio of  $L_{0.1-2.4}/L_{1-10}$ .

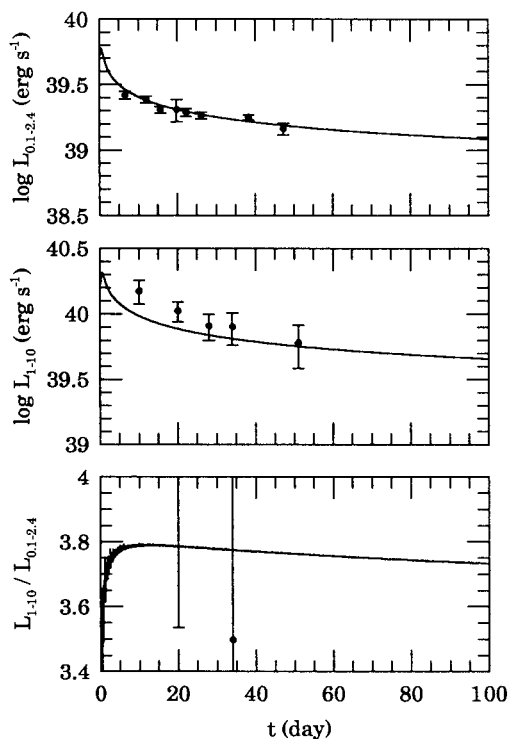


FIGURE 4. Calculated X-ray luminosities at 0.1 – 2.4 keV  $L_{0.1-2.4}$  and 1 – 10 keV  $L_{1-10}$  and their ratio  $L_{1-10}/L_{0.1-2.4}$  for the model with  $v_{\text{edge}} = 5 \times 10^4 \text{ km s}^{-1}$  and  $\rho_0 = 1 \times 10^{-14} \text{ g cm}^{-3}$ .

These comparisons show that the thermal X-rays from the shocked CSM can indeed account for the hard X-rays observed with OSSE, ASCA, and ROSAT consistently.

To reproduce the observed hardness of the X-ray emission, the expansion velocity at the outer edge of the ejecta before the collision must be fairly high ( $v_{\text{edge}} \sim 5 \times 10^4 \text{ km s}^{-1}$ ), which is consistent with a relatively low mass envelope of the progenitor, i.e., the type II-b supernova model. Soft X-rays from the shocked ejecta should be mostly absorbed, which require fairly steep density gradient of the ejecta. To reproduce the slow declines of the ROSAT curve, the CSM with  $\rho_{\text{CSM}} \propto r^{-1.8}$  leads to a better agreement, which suggests non-steady and/or asymmetric mass loss.

It should be noted that ASCA has observed iron line features (Kohmura 1994). This implies that the line forming region has a temperature of  $2\text{--}3 \times 10^8 \text{ K}$ , thus being the reverse-shocked ejecta. We speculate that a very narrow outermost layer of the ejecta had initially a shallow density gradient, thus undergoing little cooling. Certainly it is important to construct a consistent hydrodynamical model starting from more realistic configuration of the progenitor, i.e., the atmosphere with mass loss which smoothly connected with the CSM. The optical and X-ray light curves and spectra based on such a model would provide more accurate constraints on the still uncertain structures of the progenitor and the CSM. Continuing observations of X-rays with ASCA and ROSAT are highly valuable.

**Acknowledgements**

This work has been supported in part by the grant-in-Aid for Scientific Research (04640265, 05242102, 05242103, 05242207, 2539, 2780) of the Ministry of Education, Science, and Culture in Japan.

## REFERENCES

- Arnett, W. D., Bahcall, J. N., Kirshner, R. P. & Woosley, S. E. 1989, *ARA&A*, **27**, 629.
- Benz, W. 1990, In *Numerical Modeling of Nonlinear Stellar Pulsation: Problems and Prospects*, ed. Buchler, J.R., (Dordrecht: Kluwer Academic Publishers), p. 269.
- Beuermann, K., Brandt, S. & Pietsch, W. 1994, *A&A*, **281**, L45.
- Chevalier, R. A. & Luo, D. 1994, *ApJ*, **421**, 225.
- Colella, P. & Woodward, P. R. 1984, *J. Comp. Phys.*, **54**, 174.
- Gorenstein, P., Hughes, J. P. & Tucker, W. H. 1994, *ApJ*, **420**, L25.
- Hillebrandt, W. & Höflich, P. 1989, *Rep. Prog. Phys.*, **52**, 1421.
- Itoh, H., Masai, K. & Nomoto, K. 1992, In *Frontiers of X-ray Astronomy*, ed. Tanaka, Y. & Koyama, K., (Tokyo: Universal Academy Press), p. 383.
- Jakobsen, P., *et al.* 1991, *ApJ*, **369**, L63.
- Kohmura, Y. 1994, Ph.D. thesis, University of Tokyo.
- Leising, M. D., *et al.* 1994, *ApJ*, **431**, L95.
- Lundqvist, P. 1992, *PASP*, **104**, 787.
- Lundqvist, P. & Fransson, C. 1991, *ApJ*, **380**, 575.
- Luo, D. & McCray, R. 1991, *ApJ*, **379**, 659.
- Luo, D., McCray, R. & Slavin, J. 1994, *ApJ*, **430**, 264.
- Masai, K. & Nomoto, K. 1994, *ApJ*, **424**, 924.
- Nomoto, K., Shigeyama, T., Kumagai, S., Yamaoka, H. & Suzuki, T. 1993a, In *Supernovae (Les Houches Summer School, COURSE X, Session LIV)*, ed. Audouze, J. *et al.*, (Amsterdam: Elsevier Science Publishers B.V.), in press.
- Nomoto, K., Suzuki, T., Shigeyama, T., Kumagai, S., Yamaoka, H. & Saio, H. 1993b, *Nature*, **364**, 507.
- Panagia, N., Gilmozzi, R., Macchetto, F., Adorf, H.-M. & Kirshner, R. P. 1991, *ApJ*, **380**, L23.
- Podsiadlowski, Ph. 1992, *PASP*, **104**, 1.
- Shigeyama, T. & Nomoto, K. 1990, *ApJ*, **360**, 242.
- Shigeyama, T., Suzuki, T., Kumagai, S., Nomoto, K., Saio, H. & Yamaoka, H. 1994, *ApJ*, **420**, 341.
- Suzuki, T., Shigeyama, T. & Nomoto, K. 1993a, *A&A*, **274**, 883.
- Suzuki, T., Kumagai, S., Shigeyama, T., Nomoto, K., Yamaoka, H. & Saio, H. 1993b, *ApJ*, **419**, L73.
- Tanaka, Y. & the ASCA team. 1993, *IAU Circ. No.* 5753.
- Wampler, E. J., *et al.* 1990, *ApJ*, **362**, L13.
- Wang, L. & Mazzali, P. A. 1992, *Nature*, **355**, 58.
- Washimi, H., Mori, M. & Shibata, S. 1994, *Nature*, submitted.
- Woosley, S. E., Eastman, R. G., Weaver, T. A., & Pinto, P. A. 1994, *ApJ*, **429**, 300.
- Zimmermann, H.-U., *et al.* 1993, *IAU Circ. Nos.* 5748, 5750, 5766.
- Zimmermann, H.-U., *et al.* 1994, *Nature*, in press.